


Surface criticality of the antiferromagnetic Potts model

Li-Ru Zhang,¹ Chengxiang Ding ^{1,*} Youjin Deng,^{2,3} and Long Zhang^{4,†}

¹*School of Science and Engineering of Mathematics and Physics, Anhui University of Technology, Maanshan, Anhui 243002, China*

²*Department of Modern Physics, University of Science and Technology of China, Hefei, 230027, China*

³*MinJiang Collaborative Center for Theoretical Physics, College of Physics and Electronic Information Engineering, Minjiang University, Fuzhou 350108, China*

⁴*Kavli Institute for Theoretical Sciences and CAS Center for Excellence in Topological Quantum Computation, University of Chinese Academy of Sciences, Beijing 100190, China*



(Received 1 May 2022; revised 29 May 2022; accepted 1 June 2022; published 22 June 2022)

We study the three-state antiferromagnetic Potts model on the simple-cubic lattice, paying attention to the surface critical behaviors. When the nearest-neighbor interactions of the surface is tuned, we obtain a phase diagram similar to the XY model, owing to the emergent $O(2)$ symmetry of the bulk critical point. For the ordinary transition, we get $y_{h1} = 0.780(3)$, $\eta_{\parallel} = 1.44(1)$, and $\eta_{\perp} = 0.736(6)$; for the special transition, we get $y_s = 0.59(1)$, $y_{h1} = 1.693(2)$, $\eta_{\parallel} = -0.391(4)$, and $\eta_{\perp} = -0.179(5)$; in the extraordinary-log phase, the surface correlation function $C_{\parallel}(r)$ decays logarithmically with decaying exponent $q = 0.60(2)$, however, the correlation $C_{\perp}(r)$ still decays algebraically with critical exponent $\eta_{\perp} = -0.442(5)$. If the ferromagnetic next-nearest-neighbor surface interactions are added, we find two transition points, the first one is a special point between the ordinary phase and the extraordinary-log phase, the second one is a transition between the extraordinary-log phase and the Z_6 symmetry-breaking phase, with critical exponent $y_s = 0.41(2)$. The scaling behaviors of the second transition is very interesting, the surface spin-correlation function $C_{\parallel}(r)$, and the surface squared staggered magnetization at this point decays logarithmically with exponent $q = 0.37(1)$; however, the surface structure factor with the smallest wave vector and the correlation function $C_{\perp}(r)$ satisfy power-law decaying, with critical exponents $\eta_{\parallel} = -0.69(1)$ and $\eta_{\perp} = -0.37(1)$, respectively.

DOI: [10.1103/PhysRevB.105.224415](https://doi.org/10.1103/PhysRevB.105.224415)

I. INTRODUCTION

Phase transition and critical phenomena are hot topics in the research of condensed-matter and statistical physics. At the critical point of a continuous transition, the system exhibits a variety of singular behaviors characterized by algebraically decaying of correlation functions. Such types of behaviors also appear on the surface of the system and can be different to that of the bulk ones [1–5]. Depending on the strength of the surface interactions, the surface critical behavior can be classified as “ordinary transition,” “special transition,” and “extraordinary transition.” Typical examples can be found in the classical $O(n)$ models [6–8]. Generally, the ordinary transition can be found without tuning the surface interactions J_s , i.e., it is the same as the bulk ones; if it is tuned (strengthened), a phase transition may be found, which is the special point J_{sc} , and the phase with $J_s > J_{sc}$ is the extraordinary phase. It is clear that the extraordinary phases of Ising model are ordered, however, whether there is a special transition for the surface of the Heisenberg model and what the extraordinary phase is once controversial [7,9,10]. Similar problems also exist in the XY model. Until recently, the research interest in surface critical phenomena was renewed

by the exotic surface critical behavior in the quantum spin models [11–14]. A recent theoretical study pointed out that the extraordinary phase on the surface of the Heisenberg model may be an “extraordinary-log” phase characterized by logarithmically decaying of the surface correlation function [15], which has been verified numerically [16]; similar behavior is also found in the XY model [17].

The above results show that the surface critical phenomenon has many interesting characteristics, which are worth studying, and the related research are continuing [18–25]. In this paper, we study the surface critical properties of the three-state antiferromagnetic Potts model on a simple-cubic lattice [26–28]. Due to the Z_3 symmetry of the spins and the permutation symmetry of two sets of sublattices, the ground state of the system breaks the Z_6 symmetry, however, at the bulk critical point, the symmetry of the order parameter is $O(2)$, which is called “emergent $O(2)$ symmetry” [29,30], and the corresponding universality class of the phase transition is the same as the XY model. At such an emergent $O(2)$ bulk critical point, we explore the surface critical behaviors by tuning the nearest-neighbor (NN) surface interactions and the next nearest neighboring (NNN) surface interactions, the two phase diagrams we obtained are shown in Fig. 1. In the phase diagram (a), the extraordinary-log phase and the special point are obtained, which is very similar to the XY model [7,17]; we can also see that the surface cannot be ordered only by increasing the strength of the surface NN interactions, this

*dingcx@ahut.edu.cn

†longzhang@ucas.ac.cn

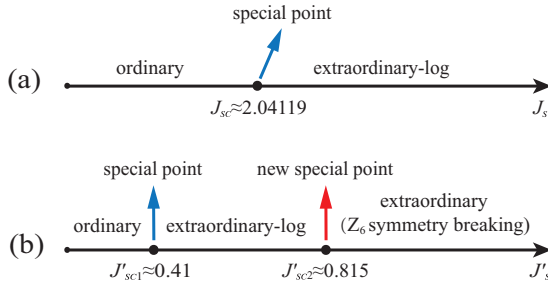


FIG. 1. Surface phase diagrams of the antiferromagnetic Potts model (1): (a) the phase diagram with NNN interactions $J'_s = 0$; (b) the phase diagram with NN interactions $J_s = 1$.

is closely related to the fact that the two-dimensional antiferromagnetic Potts model is not ordered even the temperature is down to zero [31]. However, NNN ferromagnetic interactions can induce the Z_6 symmetry-breaking phase at finite temperature for the two-dimensional antiferromagnetic Potts model [32], and this inspires us to add NNN ferromagnetic interactions to the surface of the three-dimensional antiferromagnetic Potts model; the results for this case are summarized in phase diagram (b) where a new special point with very interesting scaling behaviors is found.

The paper is arranged as follows: In Sec. II, we introduce the model and method; in Sec. III, we present the numerical results, including the refined bulk critical point, the critical behaviors about the ordinary transition, the extraordinary-log phase, and the two special points; we conclude our paper in Sec. IV.

II. MODEL AND METHOD

The antiferromagnetic Potts model we studied is defined on the simple-cubic lattice,

$$\mathcal{H} = J \sum_{\langle i,j \rangle} \delta_{\sigma_i, \sigma_j} + J_s \sum_{\langle i,j \rangle^s} \delta_{\sigma_i, \sigma_j} - J'_s \sum_{\langle\langle i,j \rangle\rangle'} \delta_{\sigma_i, \sigma_j}, \quad (1)$$

J , J_s , and J'_s are the strengths of the NN bulk interactions, the NN surface interactions, and the NNN surface interactions, respectively, noting that the NNN surface interactions are ferromagnetic. The Potts spin $\sigma_i = 1-3$, which can be mapped to a unit vector on the plane,

$$\vec{\sigma}_i = (\cos \theta_i, \sin \theta_i), \quad (2)$$

with $\theta_i = 2\pi\sigma_i/3$. Such mapping shows the symmetry of the spin, the variables we studied are based on such vectors.

The Monte Carlo algorithm we adopt is a combination of the local update (Metropolis algorithm) and a global update (cluster algorithms) [27]. For the case of $J'_s \neq 0$, the system has both antiferromagnetic and ferromagnetic interactions, the global update is a mixture of the Swendsen-Wang [33] and Wang-Swendsen-Kotecký algorithms [27]. The high efficiency of the algorithm enables us to perform simulations for the systems with sizes up to $L = 128$. In the simulations, the periodic boundary condition is applied along the x and y directions, whereas the open boundary condition is applied along the z direction.

The bulk variables we sampled include the squared (staggered) magnetization m_s^2 , the magnetic susceptibility χ_s , and the Binder ratio Q_s , which are defined as

$$m_s^2 = \langle \mathcal{M}_s^2 \rangle, \quad (3)$$

$$\chi_s = N(\langle \mathcal{M}_s^2 \rangle - \langle |\mathcal{M}_s| \rangle^2), \quad (4)$$

$$Q_s = \frac{\langle \mathcal{M}_s^2 \rangle^2}{\langle \mathcal{M}_s^4 \rangle}, \quad (5)$$

where T is the temperature and \mathcal{M}_s is defined as

$$\mathcal{M}_s = \frac{1}{N} \sum_{\vec{R}} (-1)^{x+y+z} \vec{\sigma}_{\vec{R}}. \quad (6)$$

Here $\vec{R} = (x, y, z)$ is the coordination, and $N = L^3$ is the number of sites of the lattice.

We also sample the correlation function $C(r)$ and correlation length ξ ,

$$C(r) = \langle \vec{\sigma}_i \cdot \vec{\sigma}_{i+r} \rangle, \quad (7)$$

$$\xi = \frac{(m_s^2/F - 1)^{1/2}}{2\sqrt{\sum_{i=1}^d \sin^2(\frac{k_i}{2})}}, \quad (8)$$

where \vec{k} is the “smallest wave vector” along the x direction—i.e., $\vec{k} \equiv (2\pi/L, 0, 0)$; the “structure factor” F is define as

$$F = \frac{1}{N^2} \left\langle \left| \sum_{\vec{R}} (-1)^{x+y+z} e^{i\vec{k} \cdot \vec{R}} \vec{\sigma}_{\vec{R}} \right|^2 \right\rangle. \quad (9)$$

Generally, in a critical phase, correlation ratio ξ/L assumes a universal nonzero value in the thermodynamic limit $L \rightarrow \infty$; in a disordered phase, correlation length ξ is finite, and ξ/L drops to zero, whereas in an ordered phase, ξ/L diverges quickly since the structure factor F vanishes rapidly. Therefore, similar to the Binder ratio Q_s , ξ/L is also very useful in locating the critical point of phase transition.

The definition of the surface variables are very similar to the bulk ones, but the spins in Eqs. (6), (7), and (9) should be restricted to the surface ones. For clarity, we add a subscript 1 to the surface variables, i.e., the surface squared magnetization, the surface magnetic susceptibility, the surface Binder ratio, the surface structure factor, and the surface correlation length are written as m_{s1}^2 , χ_{s1} , Q_{s1} , F_1 , and ξ_1 , respectively, except the surface correlation functions, which are written as $C_{\parallel}(r)$ and $C_{\perp}(r)$; both $C_{\parallel}(r)$ and $C_{\perp}(r)$ are calculated as Eq. (7); for $C_{\parallel}(r)$, both site i and $i+r$ are on the surface; for $C_{\perp}(r)$, site i is on the surface but site $i+r$ is in the bulk, and the line from i to $i+r$ is perpendicular to the surface.

III. RESULTS

A. Refine the bulk critical point

The simple-cubic antiferromagnetic Potts model has ever been studied by Monte Carlo simulations in Refs. [27,28], whose critical exponents coincide with the XY universality class, however, the accuracy is not very high. More accurate numerical results about the critical exponents can be found in

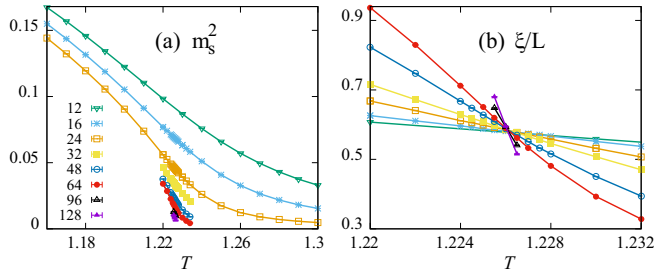


FIG. 2. Squared magnetization m_s^2 and correlation ratio ξ/L of the simple-cubic antiferromagnetic Potts model (1).

Ref. [30], whereas the interactions studied there are antiferromagnetic along the x and y directions but ferromagnetic along the z direction, such mixed interactions do not change the universality class of the phase transition but lead to a different (bulk) critical point. In the current paper, before studying the surface critical behaviors, we refine the bulk critical point for the simple-cubic antiferromagnetic model (with full antiferromagnetic interactions). As shown in Fig. 2, the bulk transition is clearly indicated by the bulk squared magnetization m_s^2 and the correlation ratio ξ/L . It can also be shown by the bulk Binder ratio Q_s , which is not shown here. In the vicinity of the critical point, ξ/L and Q_s satisfy the finite-size scaling (FSS) [34,35] formula,

$$Q = a_0 + \sum_{k=1}^{k_{\max}} a_k (T - T_c)^k L^{ky_t} + bL^{y_1}, \quad (10)$$

where Q is ξ/L or Q_s and T_c is the critical point; $y_t > 0$ is the thermal critical exponent, $y_1 < 0$ is the correction-to-scaling exponent, a_0 , a_k , and b are unknown parameters.

The data fitting of ξ/L , with fixed $y_1 = -1$, gives $T_c = 1.22603(1)$ and $y_t = 1.490(3)$; The fitting of Q_s gives $T_c = 1.22602(2)$ and $y_t = 1.483(10)$. Here we can see that although the Binder ratio is widely used in determining the critical point, it is not necessarily the best one; similar examples can also be found in Refs. [36,37]. We chose the better one $T_c = 1.22603(1)$ to be our final result, which will be used as the starting point of the study of surface critical behaviors in the next subsections. We can also see that the value of the critical exponent y_t is consistent with that of the XY universality class [38,39].

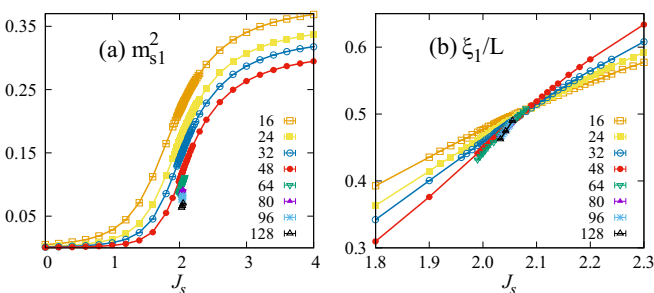


FIG. 3. Surface squared magnetization m_{s1}^2 and correlation ratio ξ_1/L of the antiferromagnetic Potts model (1) with $T = T_c^{\text{bulk}} = 1.22603$ and the NNN surface interaction $J'_s = 0$.

B. Ordinary transition

Exactly at the bulk critical point $T_c^{\text{bulk}} = 1.22603$, we perform simulations with the open boundary condition along the z direction and periodic boundary conditions along the x and y directions, and the surface interactions are set as $J_s = J = 1$ and $J'_s = 0$. In this case, the surface critical behaviors originates from the bulk correlations, which is called the ‘‘ordinary transition’’. The data of the surface squared magnetization m_{s1}^2 , the surface correlation function C_{\parallel} , the surface structure factor F_1 , and the surface correlation C_{\perp} are fit according to the scaling formulas,

$$m_{s1}^2 L^2 = c + L^{2y_{h1}-2}(a + bL^{y_1}), \quad (11)$$

$$C_{\parallel}(L/2) = L^{-1-\eta_{\parallel}}(a + bL^{y_1}), \quad (12)$$

$$F_1 L^2 = c + L^{2y_{h1}-2}(a + bL^{y_1}), \quad (13)$$

$$C_{\perp}(L/2) = L^{-1-\eta_{\perp}}(a + bL^{y_1}), \quad (14)$$

where y_{h1} , η_{\parallel} , and η_{\perp} are critical exponents; $y_1 < 0$ is the correction-to-scaling exponents; a , b , and c are unknown parameters, with c the analytical part of $m_{s1}^2 L^2$ or $F_1 L^2$, originating from the contribution of short-term correlations. Although mathematically Eqs. (11) and (13) are equivalent to

$$m_{s1}^2 = cL^{-2} + L^{2y_{h1}-4}(a + bL^{y_1}), \quad (15)$$

$$F_1 = cL^{-2} + L^{2y_{h1}-4}(a + bL^{y_1}), \quad (16)$$

respectively, technically, in the fitting of m_{s1}^2 , the right-hand side of (15) or (16) will be dominated by the first term and the fitting result of y_{h1} is often unreliable if the value of y_{h1} is smaller than 1, which is exactly the case in the ordinary transition.

The data fitting with $y_1 = -1$, gives $y_{h1} = 0.780(3)$ (from m_{s1}^2), $y_{h1} = 0.782(4)$ (from F_1), $\eta_{\parallel} = 1.44(1)$, and $\eta_{\perp} = 0.736(6)$; these values coincide with those of the XY model [7] and satisfy the scaling laws,

$$\eta_{\parallel} = d - 2y_{h1}, \quad (17)$$

$$2\eta_{\perp} = \eta_{\parallel} + \eta, \quad (18)$$

with $d = 3$ the dimension of the system and $\eta = 0.0385$ the exponent of the bulk correlation.

C. Special transition and extraordinary phase by tuning the NN surface interaction J_s

Exactly at the bulk critical point $T_c^{\text{bulk}} = 1.22603$, we tune the NN surface interaction J_s to see whether there is a special transition, this is confirmed by the behaviors of surface squared magnetization m_{s1}^2 and the surface correlation ratio ξ_1/L as shown in Fig. 3. This transition can also be detected by the Binder ratio Q_{s1} , which is not shown here. The data of ξ_1/L or Q_{s1} in the vicinity of the special point satisfy the scaling formula (10) with T replaced by J_s and the critical exponent y_t replaced by y_s ; the fitting with $y_1 = -1$ gives the critical point $J_{sc} = 2.04119(40)$ and the critical exponent $y_s = 0.59(1)$. We can see that the value of y_s is consistent with that of the XY model [7].

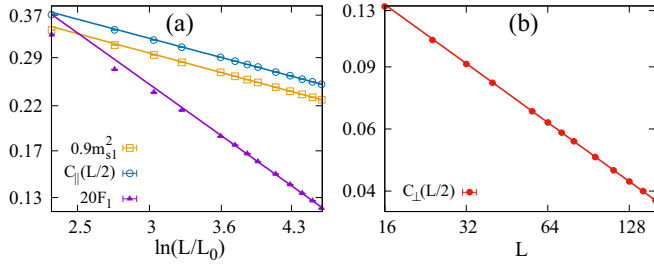


FIG. 4. (a) Log-log plot of m_{s1}^2 , $C_{||}(L/2)$, and F_1 versus $\ln(L/L_0)$ for the antiferromagnetic Potts model (1) with $T = T_c^{\text{bulk}} = 1.226\,03$, $J_s = 5$, and $J'_s = 0$; $L_0 = 1.54$ is taken for all three variables. (b) Log-log plot of the surface correlation $C_{\perp}(L/2)$.

Exactly at the special transition point $J_{sc} = 2.041\,19$, we investigate the scaling behaviors of the surface squared magnetization m_{s1}^2 , the surface correlation function $C_{||}$, the surface structure factor F_1 , and the surface correlation C_{\perp} ; they also satisfy the FSS formulas (11)–(14), respectively. Alternatively, m_{s1}^2 and F_1 can also be fit by Eqs. (15) and (16), respectively, because in the current case $y_{h1} > 1.5$, the right-hand side of the equation is dominated by the second term, whereas the first one behaves like a correction-to-scaling term. The data fitting gives $y_{h1} = 1.693(2)$ (from m_{s1}^2), $y_{h1} = 1.694(4)$ (from F_1), $\eta_{||} = -0.391(4)$, and $\eta_{\perp} = -0.179(5)$, these results coincide with those of the XY model and satisfy the scaling laws (17) and (18). For $J_s > J_{sc}$, we find that the system is in the extraordinary-log phase, characterizing by the logarithmically decaying of correlation function $C_{||}(r)$ and related variables [15–17]. Figure 4(a) shows a typical case of $J_s = 5$, and the data can be fit according to

$$m_{s1}^2 = a[\ln(L/L_0)]^{-q}, \quad (19)$$

$$C_{||}(L/2) = a[\ln(L/L_0)]^{-q}, \quad (20)$$

$$F_1 = a[\ln(L/L_0)]^{-q'}, \quad (21)$$

where q and q' are the critical exponents and a and L_0 are nonuniversal parameters. From the fitting of $C_{||}$, we get $q = 0.60(2)$ and $L_0 = 1.54(9)$; from the fitting of m_{s1}^2 and F_1 , we get $q = 0.61(1)$ and $q' = 1.61(1)$, respectively. We can see that the values of q and q' are consistent with those of the XY model [17] and satisfy the relation $q' = 1 + q$. It should be noted that in the fitting of m_{s1}^2 and F_1 , we have set the value of L_0 fixed at 1.54, such a trick is the same as that in Ref. [17] for the XY model. For the surface correlation function $C_{\perp}(L)$, we find that it is still decaying algebraically as shown in Fig. 4(b), therefore, we fit it according to Eq. (14) with $y_1 = -1$, and we get $\eta_{\perp} = -0.442(5)$.

We also study the case of $J_s = 10$ and get $q = 0.63(2)$, $q' = 1.64(2)$, $L_0 = 1.2(1)$, and $\eta_{\perp} = -0.444(7)$. The values of q and q' coincide with the cases of $J_s = 5$ and the XY model [17], which means the critical behaviors of the extraordinary-log phase of the $O(2)$ surface are universal.

In the low temperature, the order parameter of the antiferromagnetic Potts model on the simple-cubic lattice breaks the Z_6 symmetry [30], therefore, one may ask whether the surface can be ordered with such symmetry breaking when the surface

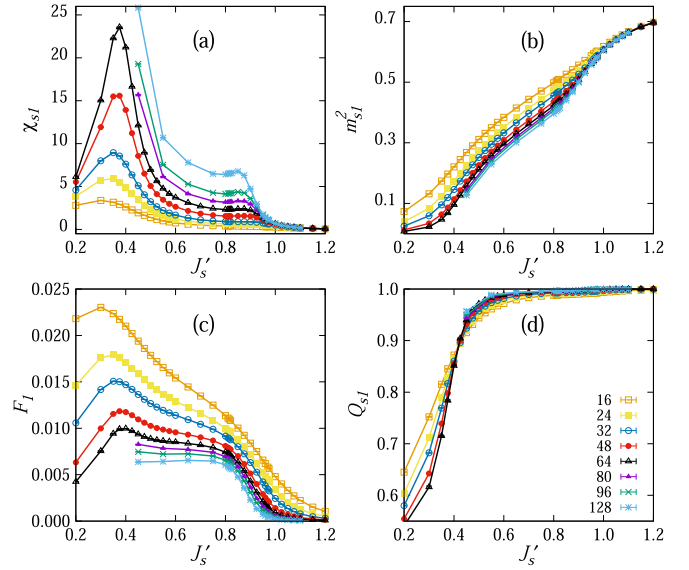


FIG. 5. Surface critical behaviors of the antiferromagnetic Potts model (1) with $T = T_c = 1.226\,03$ and $J_s = 1$: (a) surface susceptibility χ_{s1} ; (b) surface squared magnetization m_{s1}^2 ; (c) surface structure factor F_1 ; and (d) the surface Binder ratio Q_{s1} .

interactions are strengthened. However, by performing the simulations with much larger J_s , we find that the surface is always in the extraordinary-log phase, and it cannot be ordered by the strengthening of J_s . This may be related to the fact that in the limit of $J_s \rightarrow \infty$, the decoupled two-dimensional antiferromagnetic Potts model cannot be ordered even if the temperature is zero [31]. However, as we will show in the next subsection, the Z_6 symmetry-breaking surface can be reached by adding the NNN ferromagnetic interactions J'_s on the surface.

D. New special transition induced by next-nearest interactions J'_s

When the NNN ferromagnetic interactions J'_s is added to the surface, we can find two phase transitions as shown by the behaviors of the surface susceptibility χ_{s1} in Fig. 5(a). In the intermediate region $J'_{sc1} < J'_s < J'_{sc2}$ with $J'_{sc1} \approx 0.41$ and $J'_{sc2} \approx 0.85$, the scaling behaviors of χ_{s1} is very different from that in region $J'_s < J'_{sc1}$ or $J'_s > J'_{sc2}$. As we will show later, in this region, the system is in the extraordinary-log phase. Therefore, the peak of χ_{s1} at $J'_{sc1} \approx 0.41$ indicates a special transition point, similar to that studied in the above subsection. The second transition at J'_{sc2} , which we call the “new special point,” is revealed not only by the surface susceptibility χ_{s1} , but also by the surface squared magnetization m_{s1}^2 and surface structure factor F_1 as shown in Figs. 5(b) and 5(c), respectively; however, the signature of the Binder ratio Q_{s1} for this transition is not obvious as shown in Fig. 5(d).

We can see that the second peak of χ_{s1} diverges much slower than the first one, namely, the singularity of such a transition is very weak. The transition point $J'_{sc2} \approx 0.85$ is obtained by the position of such a peak of the largest system with size $L = 128$; however, considering the finite-size effect, the critical point in the thermodynamic limit should be a

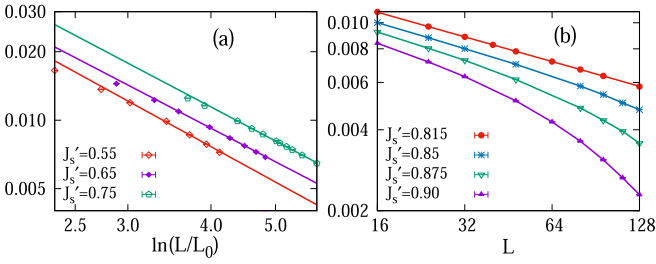


FIG. 6. (a) Log-log plot of F_1 versus $\ln(L/L_0)$ using the values of L_0 fit from m_{s1}^2 , listed in Table I; (b) log-log plot of F_1 versus L .

little smaller than this one. A more accurate estimation of the critical point can be obtained from the scaling behavior of the structure factor F_1 , which satisfies the logarithmic decaying in the region $J'_{sc1} < J'_s < J'_{sc2}$ but a power-law scaling at the transition point $J'_{sc2} = 0.815$; this is demonstrated in Fig. 6.

In the region $J'_{sc1} < J'_s < J'_{sc2}$, we check the FFS behaviors of F_1 for several cases, and the results of data fitting, according to Eq. (21), are listed in Table I. In this region, m_{s1}^2 and C_{\parallel} also satisfy the logarithmic decaying; the fitting results, according to Eqs. (19) and (20), are also listed in Table I. These results claim that in this region the system is in an extraordinary-log phase; the critical exponents q and q' in this phase are universal and satisfy the relation $q' = 1 + q$ as that in the XY model [17]. In this phase, the correlation C_{\perp} still satisfies the power-law scaling formula (14), the fitting results of η_{\perp} for several cases are also listed in Table I.

An important point should be emphasized about the extraordinary-log phase is that the surface susceptibility χ_{s1} is divergent in this phase; such a property is very different from that of the ordinary phase or the extraordinary phase with long-range order. Technically, this property can help us to detect whether a surface is in an extraordinary-log phase. It should be noted that currently, it not a trivial work to distinguish an extraordinary-log phase from a long-range ordered phase numerically without theoretical precognition especially when the value of the long-range order is relatively small.

At the transition point $J'_{sc2} = 0.815$, F_1 satisfies a power-law formula $aL^{-1-\eta_{\parallel}}$, where $\eta_{\parallel} = -0.69(1)$. The correlation function C_{\perp} also satisfies the power-law (14), and the critical exponent $\eta_{\perp} = -0.37(1)$. However, the m_{s1}^2 and C_{\parallel} at this

TABLE I. Fitting results of m_{s1}^2 , C_{\parallel} , and F_1 , where m_{s1}^2 and C_{\parallel} are fit according to Eqs. (19) and (20), respectively; F_1 is fit according to (21) when $J'_s < J'_{sc2}$ but a power-law formula $aL^{-1-\eta_{\parallel}}$ when $J'_s = J'_{sc2}$. In fitting of C_{\parallel} and m_{s1}^2 , we let L_0 free to be fit, whereas in the fitting of F_1 , we fix L_0 as that of m_{s1}^2 .

J'_s	$q(C_{\parallel})$	L_0	$q(m_{s1}^2)$	L_0	q'	η_{\perp}
0.55	0.61(3)	2.0(7)	0.59(3)	2.63(9)	1.56(4)	-0.43(1)
0.65	0.56(2)	1.36(10)	0.60(2)	0.89(5)	1.59(1)	-0.43(1)
0.75	0.55(2)	0.90(16)	0.57(1)	0.44(9)	1.57(1)	-0.38(1)
J'_{sc2}	$q(C_{\parallel})$	L_0	$q(m_{s1}^2)$	L_0	η_{\parallel}	η_{\perp}
0.815	0.37(1)	2.3(3)	0.38(1)	1.13(9)	-0.69(1)	-0.37(1)

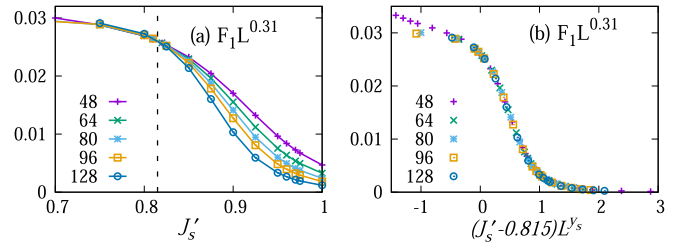


FIG. 7. (a) $F_1L^{-1-\eta_{\parallel}} = F_1L^{0.31}$ versus J'_s ; the dashed line is the critical point; (b) data collapse: $F_1L^{0.31}$ versus $(J'_s - 0.815)L^{y_s}$ with $y_s = 0.41$.

point still satisfy the logarithmically decaying formulas (19) and (20) with exponent $q = 0.37(1)$ as shown in Table I.

In the range of $J'_s > J'_{sc2}$, the surface is in a long-range ordered phase, the structure factor F_1 decays much faster, which satisfies neither a logarithmically decaying formula nor a simple power-law formula; this is also demonstrated in Fig. 6.

In order to further explore the critical behaviors of the new special point, we plot $F_1L^{-1-\eta_{\parallel}} = F_1L^{0.31}$ versus J'_s in Fig. 7(a), and we can see that $F_1L^{-1-\eta_{\parallel}}$ plays the role of a dimensionless variable, similar to the Binder ratio; Fig. 7(b) is the data collapse plot of $F_1L^{0.31}$ versus $(J'_s - 0.815)L^{y_s}$ with critical exponent $y_s = 0.41$. More rigorously, one can fit the data of F_1 in the vicinity of $J'_s = 0.815$ by the scaling formula,

$$F_1 = L^{-1-\eta_{\parallel}} \left[a_0 + \sum_{k=1}^{k_{\max}} a_k (J'_s - J'_{sc2})^k L^{ky_s} + bL^{y_1} \right], \quad (22)$$

which gives $\eta_{\parallel} = -0.69(1)$, $J'_{sc2} = 0.815(2)$, and $y_s = 0.41(2)$, these results are consistent with those applied in the data collapse in Fig. 7(b), thus, giving a self-consistent check.

To summarize, for the new special transition, it is mainly characterized by the the following critical behaviors:

$$J'_{sc2} = 0.815(2), \quad (23)$$

$$y_s = 0.41(2), \quad (24)$$

$$F_1 \sim aL^{-1-\eta_{\parallel}}, \quad \text{with } \eta_{\parallel} = -0.69(1), \quad (25)$$

$$m_{s1}^2 \sim a[\ln(L/L_0)]^{-q}, \quad \text{with } q = 0.38(1), \quad (26)$$

$$C_{\parallel} \sim a[\ln(L/L_0)]^{-q}, \quad \text{with } q = 0.37(1), \quad (27)$$

$$C_{\perp} \sim aL^{-1-\eta_{\perp}}, \quad \text{with } \eta_{\perp} = -0.37(1). \quad (28)$$

E. Symmetries of the surface

After we studied the phase transitions, we give a short description about the symmetries of the model. The three-state antiferromagnetic Potts model is well known for the emergent O(2) symmetry at the bulk critical point, although the ground state is Z_6 symmetry breaking, which is ordered by entropy. An interesting question is what the surface symmetry is.

As shown in Fig. 8, in the ordinary phase ($J'_s = 0$), the histogram visualizes the disorder properties of the surface staggered magnetization; this confirms that the surface is disorder, and the critical behaviors are purely induced by the

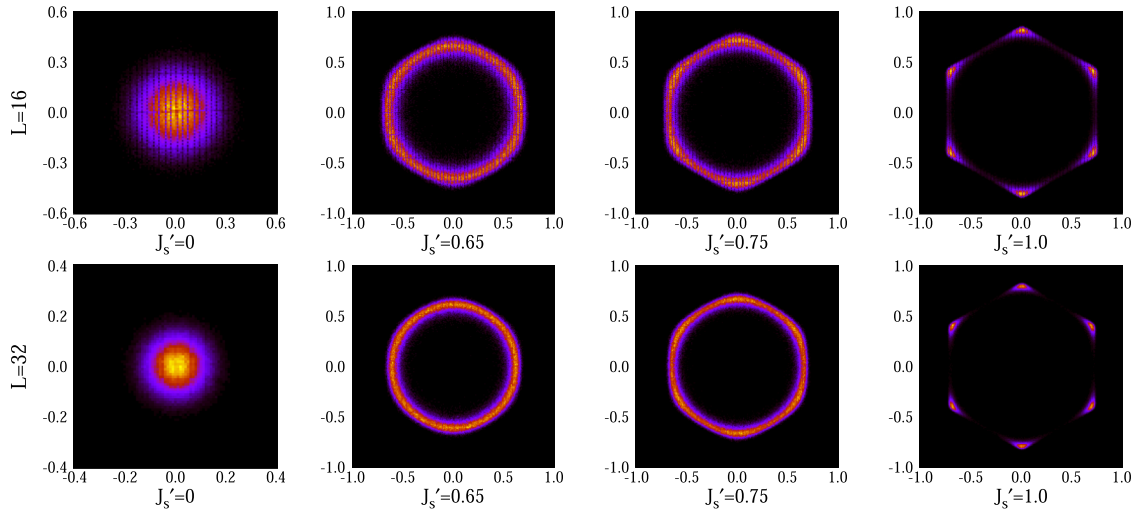


FIG. 8. Histograms of the surface staggered magnetization of the antiferromagnetic Potts model (1); in all the cases, the strength of the surface NN interactions is $J_s = 1$.

bulk criticality. For the extraordinary-log phase, we show two cases; for the case of $J'_s = 0.65$, we can see that symmetry of the order parameter is $O(2)$ when the system size reaches $L = 32$, although we can still find the shadow of the Z_6 symmetry when the system size is small ($L = 16$); for the case of $J'_s = 0.75$, we can see that the Z_6 symmetry persists to show its effect when the system size is $L = 32$, however, the effect is relatively weak comparing to that of $L = 16$, thus, we infer that in the thermodynamic limit, the symmetry should be $O(2)$. Such a property is important; it is also helpful for us to numerically distinguish the extraordinary-log phase from an ordered surface with a small value of long-range order.

When J'_s is large enough, the surface is ordered, and the Z_6 symmetry is very obvious; this is also shown in Fig. 8 with $J'_s = 1.0$.

IV. CONCLUSION AND DISCUSSION

To summarize, we have studied the surface critical behaviors of the three-state antiferromagnetic Potts model on the simple-cubic lattice; we obtain a phase diagram similar to the XY model by tuning the NN surface interactions; the universality classes of the special transition and extraordinary-log phase are the same as the XY model. A long-range-order surface which breaks the Z_6 symmetry and a new type of special transition between such an ordered phase and the extraordinary-log phase is obtained by tuning the NNN ferromagnetic surface interactions. At such a new special transition point, the scaling behaviors are very interesting; the surface squared magnetization m_{s1}^2 and the surface correlation function C_{\parallel} satisfy the logarithmic decaying with exponent $q = 0.37(1)$, but the structure factor F_1 and the correlation function C_{\perp} still satisfy the power-law decaying with critical exponents $\eta_{\parallel} = -0.69(1)$ and $\eta_{\perp} = -0.37(1)$, respectively. We also visualized the symmetries of different phases of the surface where the extraordinary-log phase is shown to conserve $O(2)$ symmetry.

We have to stress that all our conclusions about the new special transition are based on the assumption that it is a

second-order phase transition, which does not rule out the possibility of other types of phase transitions, such as the Berezinskii-Kosterlitz-Thouless (BKT) transition.

In the classical XY model, although the symmetry of the bulk critical point is also $O(2)$, the surface cannot be ordered because of the Mermin-Wagner-Hohenberg theorem [40,41], therefore, such a new type of special transition cannot appear in the classical XY model; discrete Hamiltonian symmetry and emergent $O(n)$ symmetry of bulk criticality seems a necessary condition for such a new type of special transition, such as the clock model in Ref. [43], where the new transition is detected by an angular order parameter, although the critical points are not exactly located; the FSS analysis show that in the extraordinary-log phase the scaling dimension of the Z_6 field changes continuously with the surface interactions, which is very similar to the continuous changing of critical exponents in BKT transition; however, the logarithmically decaying exponent q of the surface correlation function is still universal; consistent with the result found in the XY model [17] the result found in the current paper.

In addition to the emergent $O(2)$ critical point, other emergent $O(n)$ critical points have also been found in systems with discrete symmetry of the Hamiltonian [30,42]. It is obviously an important and interesting question to study such a new special transition and related critical properties in these models.

ACKNOWLEDGMENTS

We thank J.-P. Lv for valuable discussions and C. Xu for the advice of visualizing the symmetries of the surface by histograms. C.D. was supported by the National Science Foundation of China under Grants No. 11975024 and No. 62175001, the Anhui Provincial Supporting Program for Excellent Young Talents in Colleges and Universities under Grant No. gxyqZD2019023. L.Z. was supported by the National Key R&D Program (Grant No. 2018YFA0305800), the National Natural Science Foundation of China under Grants

No. 11804337 and No. 12174387, the CAS Strategic Priority Research Program (Grant No. XDB28000000), and the CAS Youth Innovation Promotion Association. Y.D. was supported by the National Natural Science Foundation of China

under Grant No. 11625522, the Science and Technology Committee of Shanghai under Grant No. 20DZ2210100, and the National Key R&D Program of China under Grant No. 2018YFA0306501.

-
- [1] K. Binder and P. C. Hohenberg, Surface effects on magnetic phase transitions, *Phys. Rev. B* **9**, 2194 (1974).
- [2] K. Binder, in *Phase Transitions and Critical Phenomena*, edited by C. Domb and J. L. Lebowitz (Academic, London, UK, 1983), Vol. 8.
- [3] T. C. Lubensky and M. H. Rubin, Critical phenomena in semi-infinite systems. I. ϵ expansion for positive extrapolation length, *Phys. Rev. B* **11**, 4533 (1975).
- [4] T. C. Lubensky and M. H. Rubin, Critical phenomena in semi-infinite systems. II. Mean-field theory, *Phys. Rev. B* **12**, 3885 (1975).
- [5] M. N. Barber, Scaling relations for critical exponents of surface properties of magnets, *Phys. Rev. B* **8**, 407 (1973).
- [6] M. Hasenbusch, Monte Carlo study of surface critical phenomena: The special point, *Phys. Rev. B* **84**, 134405 (2011).
- [7] Y. Deng, H. W. J. Blöte, and M. P. Nightingale, Surface and bulk transitions in three-dimensional $O(n)$ models, *Phys. Rev. E* **72**, 016128 (2005).
- [8] Y. Deng, Bulk and surface phase transitions in the three-dimensional $O(4)$ spin model, *Phys. Rev. E* **73**, 056116 (2006).
- [9] C. S. Arnold and D. P. Pappas, Gd(0001): A Semi-Infinite Three-Dimensional Heisenberg Ferromagnet with Ordinary Surface Transition, *Phys. Rev. Lett.* **85**, 5202 (2000).
- [10] M. Krech, Surface scaling behavior of isotropic Heisenberg systems: Critical exponents, structure factor, and profiles, *Phys. Rev. B* **62**, 6360 (2000).
- [11] L. Zhang and F. Wang, Unconventional Surface Critical Behavior Induced by a Quantum Phase Transition from the Two-Dimensional Affleck-Kennedy-Lieb-Tasaki Phase to a Néel-Ordered Phase, *Phys. Rev. Lett.* **118**, 087201 (2017).
- [12] C. Ding, L. Zhang, and W. Guo, Engineering Surface Critical Behavior of $(2 + 1)$ -Dimensional $O(3)$ Quantum Critical Points, *Phys. Rev. Lett.* **120**, 235701 (2018).
- [13] L. Weber, F. Parisen Toldin, and S. Wessel, Nonordinary edge criticality of two-dimensional quantum critical magnets, *Phys. Rev. B* **98**, 140403(R) (2018).
- [14] L. Weber and S. Wessel, Nonordinary criticality at the edges of planar spin-1 Heisenberg antiferromagnets, *Phys. Rev. B* **100**, 054437 (2019).
- [15] M. A. Metlitski, Boundary criticality of the $O(N)$ model in $d = 3$ critically revisited, [arXiv:2009.05119](https://arxiv.org/abs/2009.05119).
- [16] F. P. Toldin, Boundary Critical Behavior of the Three-Dimensional Heisenberg Universality Class, *Phys. Rev. Lett.* **126**, 135701 (2021).
- [17] M. Hu, Y. Deng, and J.-P. Lv, Extraordinary-Log Surface Phase Transition in the Three-Dimensional XY Model, *Phys. Rev. Lett.* **127**, 120603 (2021).
- [18] W. Zhu, C. Ding, L. Zhang, and W. Guo, Surface critical behavior of coupled Haldane chains, *Phys. Rev. B* **103**, 024412 (2021).
- [19] L. Weber and S. Wessel, Spin versus bond correlations along dangling edges of quantum critical magnets, *Phys. Rev. B* **103**, L020406 (2021).
- [20] C.-M. Jian, Y. Xu, X.-C. Wu, and C. Xu, Continuous Néel-VBS quantum phase transition in non-local one-dimensional systems with $SO(3)$ symmetry, *SciPost Phys.* **10**, 033 (2021).
- [21] F. P. Toldin and M. A. Metlitski, Boundary Criticality of the 3d $O(N)$ Model: From Normal to Extraordinary, *Phys. Rev. Lett.* **128**, 215701 (2022).
- [22] C. Ding, W. Zhu, W.-A. Guo, and L. Zhang, Special transition and extraordinary phase on the surface of a $(2 + 1)$ -dimensional quantum Heisenberg antiferromagnet, [arXiv:2110.04762](https://arxiv.org/abs/2110.04762).
- [23] X.-J. Yu, R.-Z. Huang, H.-H. Song, L. Xu, C. Ding, and L. Zhang, Conformal boundary conditions of symmetry-enriched quantum critical spin chains, [arXiv:2111.10945](https://arxiv.org/abs/2111.10945).
- [24] W.J. Zhu, C. Ding, L. Zhang, and W. Guo, Exotic surface behaviors induced by geometrical settings of two-dimensional dimerized quantum XXZ model, [arXiv:2111.12336](https://arxiv.org/abs/2111.12336).
- [25] J. Padayasi, A. Krishnan, M. A. Metlitski, I. A. Gruzberg, and M. Meineri, The extraordinary boundary transition in the 3d $O(N)$ model via conformal bootstrap, *SciPost Phys.* **12**, 190 (2022).
- [26] J. R. Banavar, G. S. Grest, and D. Jasnow, Ordering and Phase Transitions in Antiferromagnetic Potts Models, *Phys. Rev. Lett.* **45**, 1424 (1980).
- [27] J.-S. Wang, R. H. Swendsen, and R. K. Kotecký, Three-state antiferromagnetic Potts models: A monte Carlo study, *Phys. Rev. B* **42**, 2465 (1990).
- [28] C. Yamaguchi and Y. Okabe, Three-dimensional antiferromagnetic q -state Potts models: application of the Wang-Landau algorithm, *J. Phys. A* **34**, 8781 (2001).
- [29] C. Ding, W. Guo, and Y. Deng, Reentrance of Berezinskii-Kosterlitz-Thouless-like transitions in a three-state Potts antiferromagnetic thin film, *Phys. Rev. B* **90**, 134420 (2014).
- [30] C. Ding, H. W. J. Blöte, and Y. Deng, Emergent $O(n)$ symmetry in a series of three-dimensional Potts models, *Phys. Rev. B* **94**, 104402 (2016).
- [31] J. Salas and A. D. Sokal, The three-state square-lattice Potts antiferromagnet at zero temperature, *J. Stat. Phys.* **92**, 729 (1998).
- [32] M. P. M. den Nijs, M. P. Nightingale, and M. Schick, Critical fans in the antiferromagnetic three-state Potts model, *Phys. Rev. B* **26**, 2490 (1982).
- [33] R. H. Swendsen and J.-S. Wang, Nonuniversal Critical Dynamics in Monte Carlo Simulations, *Phys. Rev. Lett.* **58**, 86 (1987).
- [34] M. P. Nightingale, in *Finite-Size Scaling and Numerical Simulation of Statistical Systems*, edited by V. Privaman (World Scientific, Singapore, 1990).
- [35] M. N. Barber, in *Phase Transitions and Critical Phenomena*, edited by C. Domb and J. L. Lebowitz (Academic, New York, 1983), Vol. 8.

- [36] H. G. Katzgraber, M. Körner, and A. P. Young, Universality in three-dimensional Ising spin glasses: A Monte Carlo study, *Phys. Rev. B* **73**, 224432 (2006).
- [37] M. Hasenbusch, The binder cumulant at the Kosterlitz-Thouless transition, *J. Stat. Mech.* (2008) P08003.
- [38] Q. Liu, Y. Deng, T. M. Garoni, and H. W. J. Blöte, The $O(n)$ loop model on a three-dimensional lattice, *Nucl. Phys. B* **859**, 107 (2012).
- [39] W. Xu, Y. Sun, J.-P. Lv, and Y. Deng, High-precision Monte Carlo study of several models in the three-dimensional U(1) universality class, *Phys. Rev. B* **100**, 064525 (2019).
- [40] N. D. Mermin and H. Wagner, Absence of Ferromagnetism or Antiferromagnetism in One- or Two-Dimensional Isotropic Heisenberg Models, *Phys. Rev. Lett.* **17**, 1133 (1966).
- [41] P. C. Hohenberg, Existence of long-range order in one and two dimensions, *Phys. Rev.* **158**, 383 (1967).
- [42] F. Léonard and B. Delamotte, Critical Exponents Can Be Different on the Two Sides of a Transition: A Generic Mechanism, *Phys. Rev. Lett.* **115**, 200601 (2015).
- [43] X. Zou, S. Liu, and W. Guo, Surface critical properties of the three-dimensional clock model, [arXiv:2204.13612](https://arxiv.org/abs/2204.13612).